Hindawi Publishing Corporation
Journal of Nanomaterials
Volume 2014, Article ID 608572, 8 pages
http://dx.doi.org/10.1155/2014/608572

Research Article

Efficient Charge Transfer Mechanism in Polyfluorene/ZnO Nanocomposite Thin Films

Bandar Ali Al-Asbahi,[1,2] Mohammad Hafizuddin Haji Jumali,[1] and Rashad Al-Gaashani[3]

[1] *School of Applied Physics, Faculty of Science and Technology, Universiti Kebangsaan Malaysia (UKM), 43600 Bangi, Selangor, Malaysia*
[2] *Department of Physics, Faculty of Science, Sana'a University, Sana'a, Yemen*
[3] *Department of Physics, Thamar University, Thamar, Yemen*

Correspondence should be addressed to Bandar Ali Al-Asbahi; alasbahibandar@gmail.com
and Mohammad Hafizuddin Haji Jumali; hafizhj@ukm.my

Received 23 January 2014; Accepted 16 April 2014; Published 7 May 2014

Academic Editor: Tianxi Liu

The optical properties and charge transfer mechanism of poly (9,9′-di-n-octylfluorenyl-2.7-diyl) (PFO)/ZnO thin films have been investigated. The ZnO nanorods (NRs) were prepared via a microwave technique. The solution blending method was used to prepare the PFO/ZnO nanocomposites. X-ray diffraction (XRD) and field emission scanning electron microscope (FE-SEM) were used to determine the structural properties, while UV-Vis and photoluminescence (PL) were employed to investigate the optical properties of the films. XRD patterns confirmed that there was no variation in the structure of both PFO and ZnO NRs due to the blending process. FE-SEM micrographs displayed that ZnO NRs were well coated by PFO in all nanocomposite films. The absorption spectra of the nanocomposite thin films exhibited a red-shift indicating the increment in conjugation length of the PFO/ZnO nanocomposite. Significant quenching in the emission intensity of PFO was observed in fluorescence spectra of the nanocomposite films. This quenching was attributed to efficient charge transfer in the PFO/ZnO nanocomposites, which was further supported by the shorter PL lifetime of PFO/ZnO than that of the PFO thin film. The continuous decline in PL intensity of these nanocomposites is attributed to homogenous dynamic quenching between PFO and ZnO NRs.

1. Introduction

The growing interest in polymer based photoelectric devices, in particular conjugated polymer, can be attributed to several factors such as environmentally friendly, adjustable band gaps, high optical absorption coefficient, and low-cost fabrication. All of these factors can be achieved because of the flexibility in organic synthesis; hence, the chemical tailoring towards the desired properties is possible. For example, poly(3-hexylthiophene) and poly(p-phenylene vinylene) and their derivatives have been reported to absorb light at various wavelengths [1, 2].

There are great concerns about the photo stability and thermal stability of the polymers, although other pressing problems are associated with polymer based photoelectric devices which are poor electron-hole separation and transport properties [3, 4]. While the former concern may be overcome by introducing a more stable polymer, the later problems are more challenging. Several approaches have been suggested to inhibit these problems [5–7], but a well accepted strategy is via hybridization with inorganic semiconducting nanostructures such as metal oxides [8–11]. Successful initial attempts motivate researchers to look for the right combination between a stable polymer and metal oxide and thus their optimum ratio.

In terms of stable polymers, there are a limited number of suitable candidates and one of them is poly[9,9′-di-n-octylfluorenyl-2.7-diyl] (PFO). Earlier work reported that PFO displayed better photo stability and thermal stability than those of the poly(phenylene vinylene)s "PPVs" [12],

which are commonly studied. PFO is a semicrystalline conjugated polymer [13–15] with lowest unoccupied molecular orbital (LUMO) and highest occupied molecular orbital (HUMO) of −2.9 and −5.9 eV, respectively [16].

As one of the most widely investigated materials, ZnO is commonly used as electron acceptor in polymer/inorganic nanocomposites [17–20]. This metal oxide exhibits greater tendency to stabilize in wurtzite hexagonal form with conduction band, valence band, and energy gap of −4.2, −7.6, and 3.4 eV, respectively [18]. Most of the earlier works on polymer/ZnO nanocomposites demonstrated the photoluminescence (PL) quenching which was conveniently claimed due to efficient charge transfer effect [17–19].

One of the prerequisites for good photoelectric materials is efficient charge transfer, which in turn depends on the comparable band structures. Benefitting from quantum confinement effect with close consideration on suitability between the band structures, the combination between a more stable PFO and ZnO nanorods (NRs) is believed to result in better materials characteristics for photoelectric application. A common indicator for charge transfer is PL emission quenching. Unfortunately, observation in PL quenching alone is not sufficient to suggest efficient charge transfer. Additional evidence via measuring the fluorescence lifetime is required. However, theoretical approach via calculating fluorescence lifetime [21] is conveniently used as an alternative method especially for researchers having limited equipment at their disposal. The current work is not only calculated fluorescence lifetime, but also other important parameters, namely, the quenching rate constant [22] and photo-induced electron transfer rate [23], which are used together as supplementary evidence to indicate tendencies of determined systems.

Evidence for charge transfer in PFO/ZnO nanocomposites primarily from PL quenching was demonstrated in this work. In addition, values for the aforementioned parameters in case of dry thin films at room temperature were calculated to provide additional evidence for the effective charge transfers. The quenching type and quenching efficiency were also determined in order to have more comprehensive information on the suitability of this nanocomposite as an active layer in the photoelectric devices.

2. Experimental Details

ZnO NRs were synthesized using the microwave technique. A microwave oven (Sanyo Electric model no. EM-G430, 2.45 GHz, 1000 W) was used in this work. Deionized water (resistivity 18.2 MΩ·cm) was used to prepare zinc acetate dihydrate 0.15 M ($C_4H_6O_4Zn{\cdot}2H_2O$) (Aldrich, Fluka) aqueous solution (A) and 3.33 M of NaOH aqueous solution (B) at room temperature. The zinc acetate aqueous solution (A) was stirred for 5 min and then the aqueous solution (B) was added dropwise under steady stirring until a white solution was formed. Then, the final white solution was exposed to microwave radiation in the oven for 5 min before being left to cool naturally to 30°C. Subsequently, the solution was centrifuged at 4000 rpm for 5 min to collect the white precipitate produced after radiation. The precipitate was washed with alcohol and deionized water alternately for four times and then was dried under atmosphere at 60°C for 24 h. Finally, the obtained powder was heated at 500°C for 2 h in a conventional oven.

The PFO (product from Sigma Aldrich, USA) with average molecular weight of 58.200 was used in this study. To prepare the nanocomposites, firstly, the PFO was dissolved in tetrahydrofuran (THF) at a concentration of 3.0 mg/mL (PFO/THF). The PFO/ZnO nanocomposites were prepared in solution form by blending the fixed concentration of ZnO (3.0 mg/mL) with various ratios of PFO (0, 10, 30, 50, and 70 wt.%) followed by sonication for 5 min. Then, the solution was deposited onto a glass substrate (1.2 cm × 2 cm) to form three layers by a spin coating technique (rotational speed of 2000 rpm for 30 s). Finally, it was left to dry at room temperature.

The structural characterization of the films was carried out by X-ray diffraction (Bruker-AXS D8 Advance X-ray diffractometer using Cu-Kα radiation source with λ = 1.5418 Å). The nanostructure of the films was observed using a field emission scanning electron microscope (FE-SEM) model Supra 55VP with operating voltage of 3.00 kV. The absorption and emission spectra of the films were recorded using UV-Vis spectrophotometer (Perkin Elmer LAMBDA 900) and Luminescence spectrometer (Perkin Elmer LS55), respectively.

3. Results and Discussion

The X-ray diffractograms for the ZnO NRs, PFO, and PFO/ZnO nanocomposite thin films are shown in Figure 1. The diffractogram of ZnO NRs shows that all peaks can be indexed to the wurtzite hexagonal structure of ZnO crystal and no other crystalline peaks of any impurities were detected (Figure 1(a)). By comparison, the XRD diffractograms for PFO consist of a narrow peak at 7° and broad peaks in between 10° and 30° (2θ), which can be deconvoluted into three broad peaks at 15.5°, 20.0°, and 23.1°. This observation confirmed that the PFO is in semicrystalline phase as suggested by earlier reports [13–15]. The X-ray diffractograms for nanocomposite thin films consist of broad PFO peaks with several narrow peaks representing ZnO NRs. The intensities of ZnO NRs peaks in these nanocomposite films are enhanced as more ZnO NRs are added into the polymer (Figure 1(c)). More importantly, the structure of both PFO and ZnO NRs remained unchanged even after the blending process.

Figure 2 displays the morphology of ZnO NRs and PFO/ZnO nanocomposites. The ZnO existed as wurtzite hexagonal nanorods (pencil-like) having an average diameter of about 95 nm and length of 800 nm (Figure 2(a)). The nanorods were closely packed which were grown from a common seed. The smooth hexagonal structures of the ZnO NRs confirm that the nanorods were well crystalline as wurtzite unit cell.

The general view of nanocomposite film (Figure 2(b)) reveals the uniformity of the deposited film. A closer view of

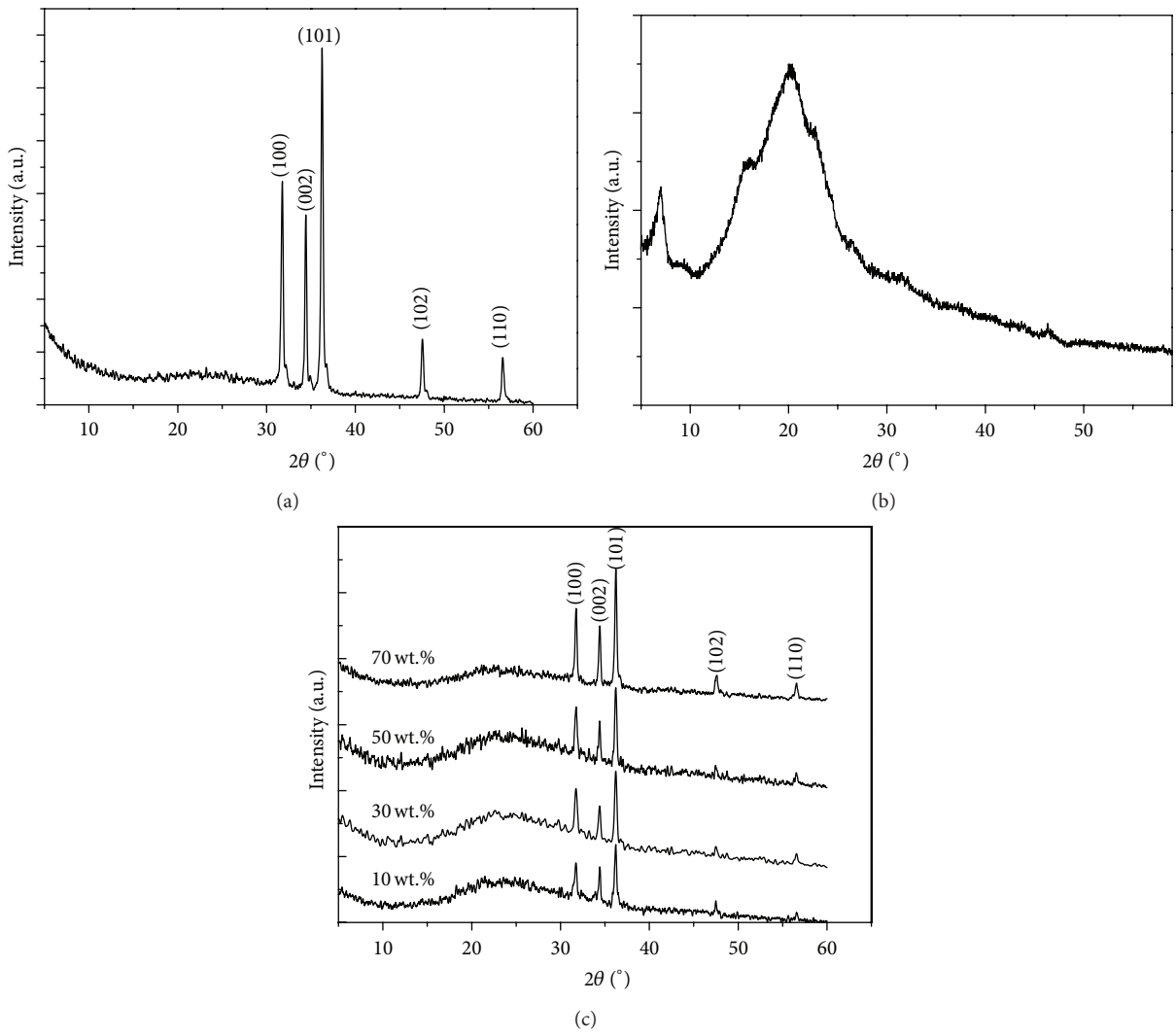

Figure 1: XRD patterns of (a) ZnO NRs, (b) pure PFO, and (c) PFO/ZnO nanocomposite films.

the films showed that the majority of ZnO NRs were broken into smaller rods and covered by PFO in all nanocomposites thin films (Figures 2(c)–2(f)). At 10 wt.% ZnO NRs, all nanorods were covered and uniformly distributed. As the ZnO NRs content increased, the nanorods were thinly coated by the PFO. At 70 wt.%, there were many uncoated nanorod bundles, which are believed to be due to the lack of PFO.

The absorption spectra of all films were presented in Figure 3. The UV-Vis spectrum of PFO film displays a λ_{max} at 404 nm which corresponds to a Π-Π^* transition [24] and a shoulder around 435 nm as the fingerprint for β-phase of PFO [25]. By comparison, the absorption edge of ZnO NRs was located in the UV region (<360 nm), which is similar to an earlier report [21]. Upon addition of ZnO NRs, the absorbance of the nanocomposite films was dramatically reduced. No additional absorption peak was observed in the spectra confirming the absence of interaction between PFO and ZnO NRs at the ground states [19].

Relative to pure PFO, all absorption peaks of PFO/ZnO nanocomposite thin films were red-shifted (around 11 nm) signifying the extension in the conjugation length of the nanocomposites [26–28].

Figure 4 shows the fluorescence spectra of ZnO NRs, pure PFO, and PFO/ZnO nanocomposite thin films with various ZnO contents. The UV emission in the fluorescence spectrum of ZnO NRs (Figure 4(a)) comprises two overlapping bands. The peak of the first band centered at 378 nm, which is related to the near-band edge emission of the wide band gap ZnO NRs. This band was due to the recombination of excitonic centres in the nanorod [29]. Additionally, a broad green band at 460–550 nm was observed, which is mainly caused by the intrinsic defects or oxygen vacancies in the ZnO NRs and results in the recombination of a photo-generated hole with the single ionized charge state of this defect [21, 30].

Figure 4(b) reveals the emission peaks of PFO at 427, 442, 465, and 500 nm, which were assigned to 0-0, 0-1, 0–2, and 0–3 vibronic transition, respectively. As in absorption spectra, addition of ZnO NRs resulted in red-shift of the emission peaks position. More importantly, a dramatic quenching of PFO emission intensity was observed, and above 30 wt.% of

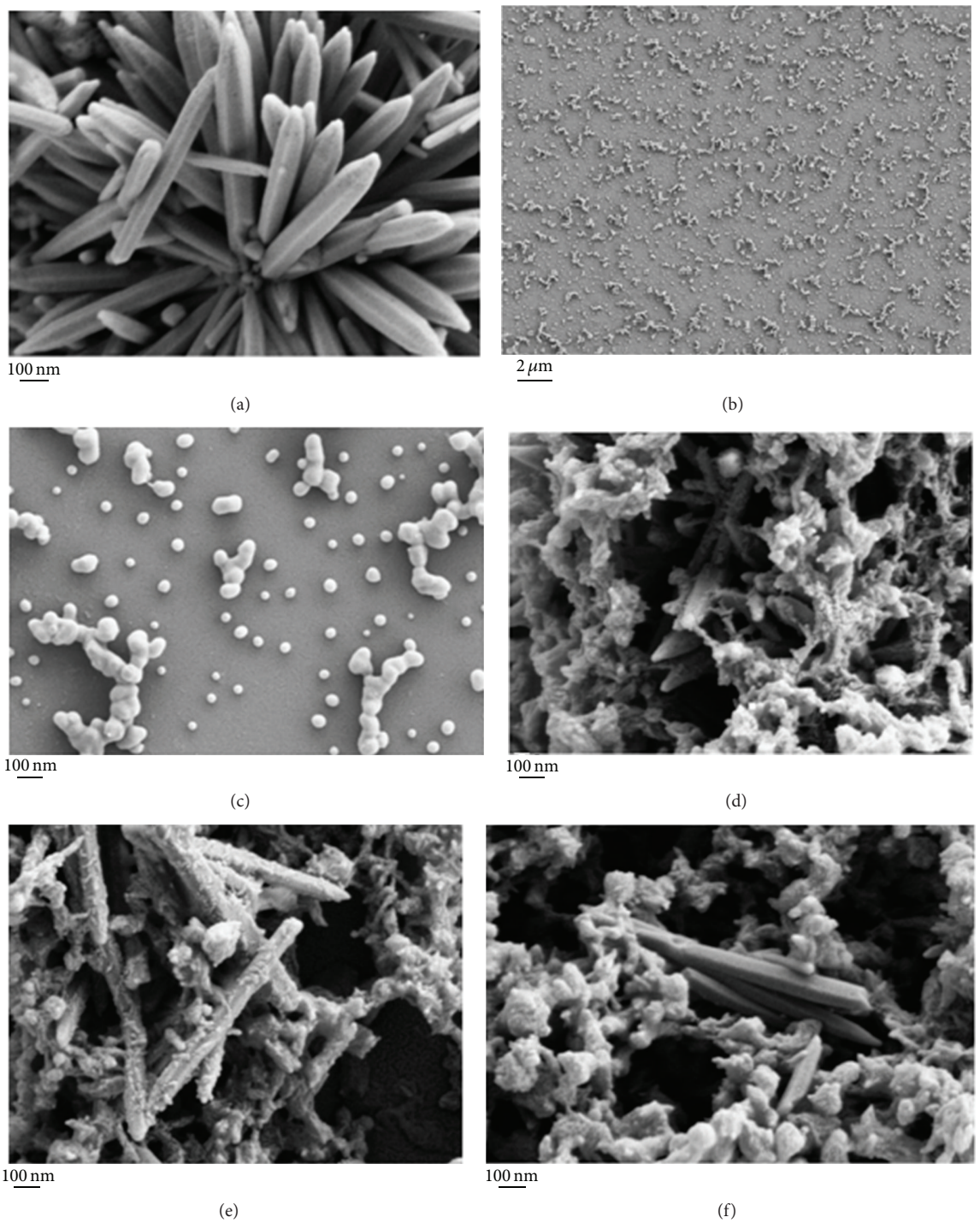

Figure 2: FE-SEM images of ZnO NRs and PFO/ZnO nanocomposites: (a) ZnO NRs, (b) distribution of PFO/ZnO nanocomposite on thin film at 90 : 10 wt.%, (c) 90 : 10 wt.%, (d) 70 : 30 wt.%, (e) 50 : 50 wt.%, and (f) 30 : 70 wt.% nanocomposite thin films.

ZnO NRs content, the 427 nm peak of pure PFO completely disappeared.

Since there was no overlap between the emission spectrum of PFO (Figure 4(b)) and the absorption spectrum of ZnO NRs (Figure 3(a)), dramatic PL quenching in PFO in the hybrid system was due to charge transfer from the polymer to the metal oxide NRs [31]. Due to the presence of ZnO NRs, recombination of exciton in PFO was inhibited. Instead, the electron-hole pairs in the polymer dissociated at the PFO/ZnO interface with the electrons moving across the interface into ZnO NRs while the holes remain in the PFO.

This argument is supported by the fact that the conduction and valence bands of ZnO are relatively lower than those of PFO. Therefore, from an energy level point of

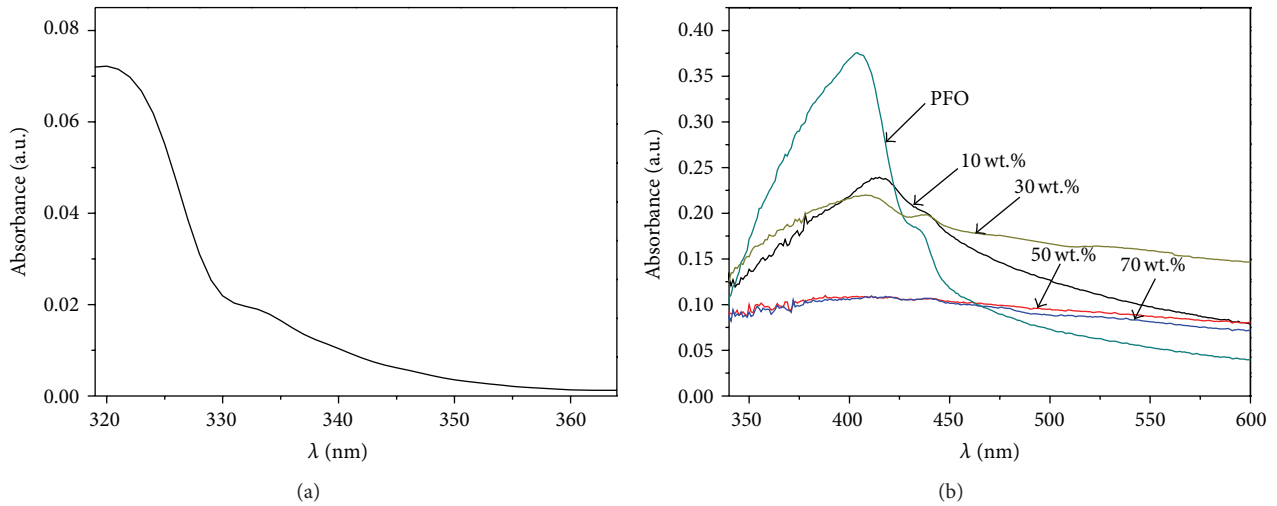

Figure 3: Absorption spectra of PFO/ZnO nanocomposite films.

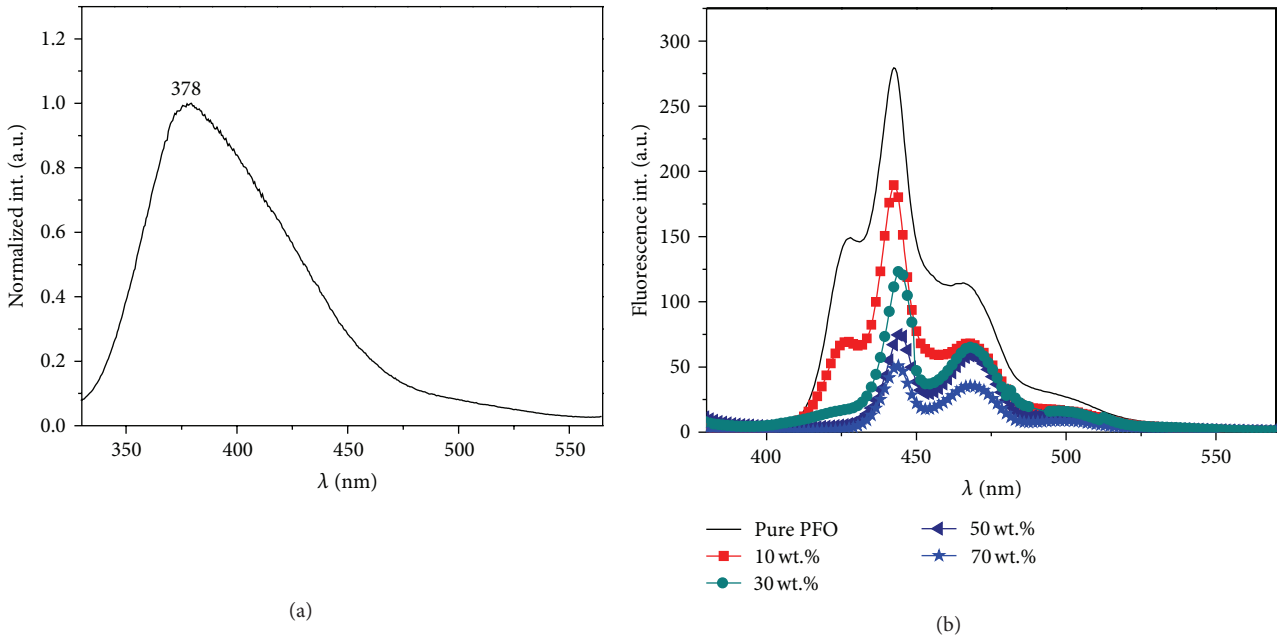

Figure 4: Fluorescence spectra of (a) pure ZnO NRs, excitation at 320 nm, and (b) pure PFO and PFO/ZnO nanocomposite films, excitation at 355 nm.

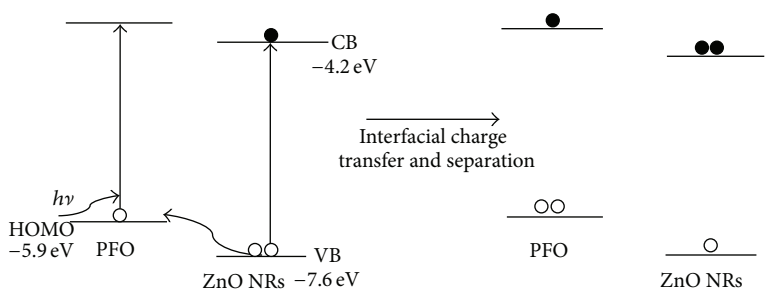

Figure 5: The interfacial charge generation, transfer, and separation between PFO and ZnO NRs. (Open circle: hole; closed circle: electron).

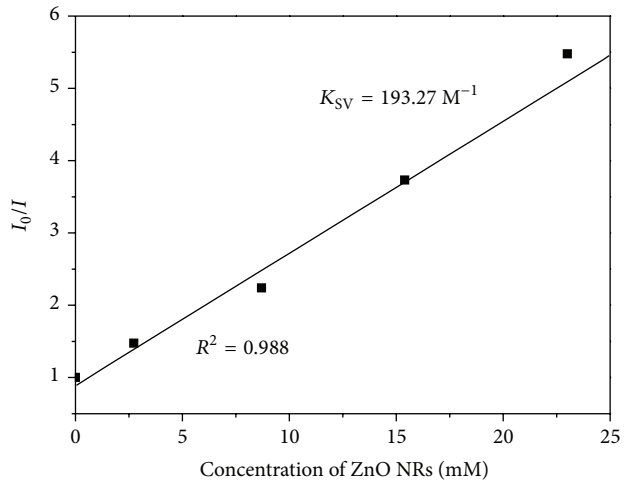

Figure 6: Stern-Volmer plot for fluorescence quenching of 3 mg/mL (PFO) by ZnO NRs.

view, the effective transfer of electron across the interface is possible (Figure 5). The dissociation of electron-hole pairs at interface and subsequent efficient electrons transfer to ZnO NRs suggested that the PFO/ZnO nanocomposite is a promising p-n-type nanocomposite material.

Effective charge transfer between PFO and ZnO NRs can be further confirmed from important parameters such as quenching rate constant (K_{SV}), lifetime (τ) of excited PFO in the presence of ZnO NRs, bimolecular quenching rate (k_q), and photo-induced electron transfer rate (K_{ET}). K_{SV} is the value of the slope in Stern-Volmer plot. The τ, k_q, and K_{ET} can be calculated once the K_{SV} value is obtained.

Utilizing Stern-Volmer relationship [22], a linear Stern-Volmer plot with $R^2 = 0.988$ can be drawn and presented in Figure 6. The linear relationship is a very important indicator of homogenous dynamic quenching of this hybrid material. The slop of the plot was ~193.27 M^{-1}, which was comparable with MEH-PPV/TiO_2 nanocomposite material [31]. This K_{SV} value signified that 50% of the PFO emission quenched at ZnO NRs concentration of 5.2 mM.

In homogeneous dynamic quenching, the Stern-Volmer equation can be rewritten as [22]

$$\frac{\tau_0}{\tau} = 1 + K_{SV}[Q], \quad (1)$$

where τ and τ_0 are the excited state lifetime of PFO in the presence and absence of ZnO NRs, respectively, and [Q] is the concentration of ZnO NRs.

Table 1 shows the effect of quencher (ZnONRs) on the photoluminescence lifetime of PFO. All nanocomposite materials exhibited shorter lifetime than the pristine PFO thin film, $\tau_0 = 0.346$ ns [32] confirming the efficient charge transfer from PFO to ZnO NRs at the interfaces [21]. Furthermore, compatible band structure between both materials induced the electron transfer from LUMO of PFO to CB of ZnO (Figure 5).

The bimolecular quenching rate (k_q) and the photo-induced electron transfer rate (K_{ET}) for PFO/ZnO nanocomposite films can be calculated using (2) [33] and (3) [34] as follows:

$$K_{SV} = \tau_0 k_q \quad (2)$$

$$K_{ET} = \frac{1}{\tau} - \frac{1}{\tau_0}. \quad (3)$$

Using (2), the k_q has been evaluated as 5.59×10^{11} M^{-1}·S^{-1}. This value is significantly greater than the minimum value for efficient quenching, which is 1×10^{10} M^{-1}·S^{-1} [22]. The high value of k_q obtained in this work proves the good combination between the ZnO NRs and PFO. Equally important, high k_q value signified the admirable quality of the interface between these two materials. The values of k_{ET} calculated using (3) were constantly increased from 1.53×10^9 to 12.73×10^9 S^{-1} as more ZnO NRs are added into PFO (Table 1). This finding provides additional evidence illustrating significant improvement in quenching efficiency and charge transfer in PFO/ZnO nanocomposite upon increment of ZnO NRs. The calculated k_{ET} values in this work are comparable with other organic-metal oxide nanocomposite systems such as phycocyanin/TiO_2 [23]. In other words, the photo-induced electron transfer rate from PFO monomers to ZnO NRs can be controlled with the ZnO NRs content. High ZnO NRs content has a high surface area, which gives an increase to a lot of defects and raises the electron transfer rate. Consequently, more efficient PFO/ZnO nanocomposite can be obtained as an active layer in photoelectric devices.

4. Conclusion

This work reports on the study of charge transfer mechanism in PFO/ZnO nanocomposite thin films. ZnO NRs were successfully synthesized using the microwave technique, whereas PFO/ZnO nanocomposites were successfully prepared via solution blending method prior to producing the films using spin coating technique. The X-ray diffractograms confirmed the purity of ZnO NRs and the existence of amorphous phase of PFO and crystalline phase of ZnO NRs. As the ZnO NRs content increased, the emission intensity of PFO reduced suggesting enhanced quenching fluorescence of PFO. The quenching rate (K_{SV}) and the bimolecular quenching rate (K_q) constants were estimated to be about 193.27 M^{-1} and 5.59×10^{11} M^{-1}·S^{-1}, respectively. In addition, as the ZnO NRs content increased from 10 to 70 wt.%, the photo-induced electron transport rate increased from 1.53×10^9 to 12.73×10^9 S^{-1}. Moreover, it was found that the photoluminescence lifetime for the PFO/ZnO thin films is much shorter than that of the pure PFO thin film. These findings confirmed the efficient electron transfer across PFO/ZnO interface, which are very crucial for greater improvement in the performance of the PFO/ZnO based photoelectric devices.

Table 1: Photo-induced electron transport rate and lifetime values of PFO/ZnO nanocomposite thin films.

The weight ratio of ZnO NRs (wt.%)	Concentration of ZnO NRs [Q] (mM)	Lifetime of PFO τ (ns)	Photo-induced electron transport rate K_{ET} (S^{-1}) $\times 10^9$
0	0	0.346	—
10	2.73	0.226	1.53
30	8.7	0.129	4.86
50	15.4	0.087	8.60
70	23.0	0.064	12.73

Conflict of Interests

The authors declare that they have no conflict of interests regarding the publication of this paper.

Acknowledgment

The authors would like to thank the Universiti Kebangsaan Malaysia (UKM) for providing excellent research facilities, under the Research University Grants DPP-2013-048 and DLP-2013-012.

References

[1] F. Padinger, R. S. Rittberger, and N. S. Sariciftci, "Effects of postproduction treatment on plastic solar cells," *Advanced Functional Materials*, vol. 13, no. 1, pp. 85–88, 2003.

[2] Q. Zhou, Q. Hou, L. Zheng, X. Deng, G. Yu, and Y. Cao, "Fluorene-based low band-gap copolymers for high performance photovoltaic devices," *Applied Physics Letters*, vol. 84, no. 10, pp. 1653–1655, 2004.

[3] W. U. Huynh, J. J. Dittmer, and A. P. Alivisatos, "Hybrid nanorod-polymer solar cells," *Science*, vol. 295, no. 5564, pp. 2425–2427, 2002.

[4] D. Haarer, "Photoconductive polymers: structure, mechanisms, and properties," *Die Angewandte Makromolekulare Chemie*, vol. 183, no. 1, pp. 197–220, 1990.

[5] S. R. Forrest, "The road to high efficiency organic light emitting devices," *Organic Electronics: Physics, Materials, Applications*, vol. 4, no. 2-3, pp. 45–48, 2003.

[6] F. Li, Y. Du, Y. Chen, L. Chen, J. Zhao, and P. Wang, "Direct application of P3HT-DOPO@ZnO nanocomposites in hybrid bulk heterojunction solar cells via grafting P3HT onto ZnO nanoparticles," *Solar Energy Materials and Solar Cells*, vol. 97, pp. 64–70, 2012.

[7] T. P. Nguyen, C. W. Lee, S. Hassen, and H. C. Le, "Hybrid nanocomposites for optical applications," *Solid State Sciences*, vol. 11, no. 10, pp. 1810–1814, 2009.

[8] J. K. Lee, W. L. Ma, C. J. Brabec et al., "Processing additives for improved efficiency from bulk heterojunction solar cells," *Journal of the American Chemical Society*, vol. 130, no. 11, pp. 3619–3623, 2008.

[9] A. J. Moulé and K. Meerholz, "Controlling morphology in polymer-fullerene mixtures," *Advanced Materials*, vol. 20, no. 2, pp. 240–245, 2008.

[10] N. Z. Yahya and M. Rusop, "Investigation on the optical and surface morphology of conjugated polymer MEH-PPV: ZnO nanocomposite thin films," *Journal of Nanomaterials*, vol. 2012, Article ID 793679, 4 pages, 2012.

[11] M. Alam, N. M. Alandis, A. A. Ansari, and M. R. Shaik, "Optical and electrical studies of polyaniline/ZnO nanocomposite," *Journal of Nanomaterials*, vol. 2013, Article ID 157810, 5 pages, 2013.

[12] A. M. Assaka, P. C. Rodrigues, A. R. M. de Oliveira et al., "Novel fluorine containing polyfluorenes with efficient blue electroluminescence," *Polymer*, vol. 45, no. 21, pp. 7071–7081, 2004.

[13] G. C. Farial, T. S. Plivelic, R. F. Cossiello et al., "A multitechnique study of structure and dynamics of polyfluorene cast films and the influence on their photoluminescence," *Journal of Physical Chemistry B*, vol. 113, no. 33, pp. 11403–11413, 2009.

[14] M. H. H. Jumali, B. A. Al-Asbahi, C. C. Yap, M. M. Salleh, and M. S. Alsalhi, "Optoelectronic property enhancement of conjugated polymer in poly(9,9′-di-n-octylfluorenyl-2.7-diyl)/titania nanocomposites," *Thin Solid Films*, vol. 524, pp. 257–262, 2012.

[15] M. H. H. Jumali, B. A. Al-Asbahi, C. C. Yap, M. M. Salleh, and M. S. Alsalhi, "Optical properties of poly (9,9′-di-n-octylfluorenyl-2.7-diyl)/amorphous SiO_2 nanocomposite thin films," *Sains Malaysiana*, vol. 42, no. 8, pp. 1151–1157, 2013.

[16] M. Bajpai, R. Srivastava, M. N. Kamalasanan, R. S. Tiwari, and S. Chand, "Charge transport and microstructure in PFO:MEH-PPV polymer blend thin films," *Synthetic Metals*, vol. 160, no. 15-16, pp. 1740–1744, 2010.

[17] I. Park, Y. Lim, S. Noh et al., "Enhanced photovoltaic performance of ZnO nanoparticle/poly(phenylene vinylene) hybrid photovoltaic cells by semiconducting surfactant," *Organic Electronics: Physics, Materials, Applications*, vol. 12, no. 3, pp. 424–428, 2011.

[18] L. Qian, Y. Zheng, K. R. Choudhury et al., "Electroluminescence from light-emitting polymer/ZnO nanoparticle heterojunctions at sub-bandgap voltages," *Nano Today*, vol. 5, no. 5, pp. 384–389, 2010.

[19] R. Jetson, K. Yin, K. Donovan, and Z. Zhu, "Effects of surface modification on the fluorescence properties of conjugated polymer/ZnO nanocomposites," *Materials Chemistry and Physics*, vol. 124, no. 1, pp. 417–421, 2010.

[20] K. Yuan, F. Li, L. Chen, and Y. Chen, "Approach to a block polymer precursor from poly(3-hexylthiophene) nitroxide-mediated in situ polymerization for stabilization of poly(3-hexylthiophene)/ZnO hybrid solar cells," *Thin Solid Films*, vol. 520, no. 19, pp. 6299–6306, 2012.

[21] Y. Y. Lin, C. W. Chen, W. C. Yen, W. F. Su, C. H. Ku, and J. J. Wu, "Improved performance of polymer/TiO_2 nanorod bulk heterojunction photovoltaic devices by interface modification," *Applied Physics Letters*, vol. 92, no. 5, Article ID 053312, 4 pages, 2008.

[22] J. R. Lakowicz, *Principles of Fluorescence Spectroscopy*, Springer, New York, NY, USA, 3rd edition, 2008.

[23] A. Kathiravan and R. Renganathan, "Photosensitization of colloidal TiO_2 nanoparticles with phycocyanin pigment," *Journal of Colloid and Interface Science*, vol. 335, no. 2, pp. 196–202, 2009.

[24] Z. Han, J. Zhang, X. Yang, H. Zhu, and W. Cao, "Synthesis and application in solar cell of poly(3-octylthiophene)/titania nanotubes composite," *Organic Electronics: Physics, Materials, Applications*, vol. 11, no. 8, pp. 1449–1460, 2010.

[25] R. Palacios, P. Formentin, E. Martinez-Ferrero, J. Pallarès, and L. F. Marsal, "β-phase morphology in ordered poly(9,9-dioctylfluorene) nanopillars by template wetting method," *Nanoscale Research Letters*, vol. 6, no. 1, pp. 1–5, 2011.

[26] G. Chen and P. Wang, "Alteration of the optical properties of poly 9,9′-dioctylfluorene by TiO_2 nanocrystalline," *Journal of Non-Crystalline Solids*, vol. 352, no. 23–25, pp. 2536–2538, 2006.

[27] T. W. Hagler, K. Pakbaz, K. F. Voss, and A. J. Heeger, "Enhanced order and electronic delocalization in conjugated polymers oriented by gel processing in polyethylene," *Physical Review B*, vol. 44, no. 16, pp. 8652–8666, 1991.

[28] K. Pichler, D. A. Halliday, D. D. C. Bradley, P. L. Burn, R. H. Friend, and A. B. Holmes, "Optical spectroscopy of highly ordered poly(p-phenylene vinylene)," *Journal of Physics: Condensed Matter*, vol. 5, no. 38, pp. 7155–7172, 1993.

[29] M. H. Huang, Y. Wu, H. Feick, N. Tran, E. Weber, and P. Yang, "Catalytic growth of zinc oxide nanowires by vapor transport," *Advanced Materials*, vol. 13, no. 2, pp. 113–116, 2001.

[30] D. K. Bhat, "Facile synthesis of ZnO nanorods by microwave irradiation of zinc-hydrazine hydrate complex," *Nanoscale Research Letters*, vol. 3, no. 1, pp. 31–35, 2008.

[31] T. Vats, S. N. Sharma, M. Kumar et al., "Comparison of photostability, optical and structural properties of TiO_2/conjugated polymer hybrid composites prepared via different methods," *Thin Solid Films*, vol. 519, no. 3, pp. 1100–1105, 2010.

[32] B. A. Al-Asbahi, M. H. H. Jumali, C. C. Yap, M. H. Flaifel, and M. M. Salleh, "Photophysical properties and energy transfer mechanism of PFO/Fluorol 7GA hybrid thin films," *Journal of Luminescence*, vol. 142, pp. 57–65, 2013.

[33] F. Ricchelli, "Photophysical properties of porphyrins in biological membranes," *Journal of Photochemistry and Photobiology B: Biology*, vol. 29, no. 2-3, pp. 109–118, 1995.

[34] J. Zimmermann, J. von Gersdorff, H. Kurreck, and B. Röder, "Determination of the electron transfer parameters of a covalently linked porphyrin-quinone with mesogenic substituents—optical spectroscopic studies in solution," *Journal of Photochemistry and Photobiology B: Biology*, vol. 40, no. 3, pp. 209–217, 1997.